

# Intensity-modulated, stepped frequency cw lidar for distributed aerosol and hard target measurements

Marc L. Simpson, Meng-Dawn Cheng, Thang Q. Dam, Katey E. Lenox, Jeff R. Price, John M. Storey, Eric A. Wachter, and Walt G. Fisher

A compact frequency-modulated, continuous wave (FM-cw) lidar system for measurement of distributed aerosol plumes and hard targets is presented. The system is based on intensity modulation of a laser diode and quadrature detection of the return signals. The advantages of using laser diode amplitude modulation and quadrature detection is a large reduction in the hardware required for processing and storing return signals as well as the availability of off-the-shelf integrated electronic components from the wireless and telecommunication communities. Equations to invert the quadrature signal components and determine spatial distributions of multiple targets are derived. Spatial scattering intensities are used to extract aerosol backscatter coefficients, which can then be directly compared to microphysics aerosol models for environmental measurements. Finally, results from laboratory measurements with a monostatic FM-cw lidar system with both hard targets and aerosols are discussed. © 2005 Optical Society of America

OCIS codes: 010.3640, 280.1100, 290.5820, 290.5850.

## 1. Introduction

The development of a small, compact light detection and ranging (lidar) system based on intensity modulation is part of an ongoing effort at Oak Ridge National Laboratory to develop prototype instruments to remotely and nonintrusively measure  $\text{NO}_x$  and particulate matter emissions from heavy trucks in motion.<sup>1</sup> Lidar is an instrument that has been used for decades to determine distance to a target and to measure aerosol distributions in the earth's atmosphere. The general approach is simple, but implementation and interpretation of data in real-world measurements are often quite complex. In conventional time-of-flight (TOF) lidar, a narrow laser pulse is transmitted toward a target. The target scatters the laser pulse, and a portion of the scattered light returns to the instrument. The timing between departure and arrival of pulses then determines dis-

tance to the target. A TOF or pulsed lidar is well suited for the measurement of distance to a specular, or hard, target. For pulsed lidar, spatial resolution is given by  $c\tau/2$ , where  $c$  is the speed of light and  $\tau$  is the pulse width. Pulsed lidar is also frequently used in conventional distributed atmospheric measurements (e.g., aerosols in the troposphere) with 100 m spatial resolution over kilometers of unambiguous range and results in practical systems with  $>10$  ns pulse width, low-repetition-rate lasers, and megahertz electronics. The measurement of localized, rapidly changing distributed targets, such as anthropogenic aerosols, however, can require tens of centimeters' spatial resolution for distances of tens of meters. For conventional pulsed lidar, these requirements translate into exotic (and expensive) high-repetition-rate, subnanosecond pulsed lasers with gigahertz electronics.

Several pulsed lidar systems are now being developed based on traditional TOF lidar for which the emphasis is on solid-state near-infrared microlasers with narrow pulse widths. One example of a solid-state TOF lidar system uses a 3 mJ solid-state (Nd:YAG) laser shifted to 1.5  $\mu\text{m}$  (with an optical parametric oscillator crystal) that operates over an unambiguous range of 3 km in clear air.<sup>2</sup> The laser has a 27 ns pulse width (4.1 m spatial resolution) at a 15 s repetition interval in a 3 mm  $\times$  3 mm  $\times$  50 mm package. The receiver is an InGaAs pin photodiode, and the laser is pumped by a commercial

---

M. L. Simpson (simpsonml@ornl.gov), M. D. Cheng, T. Q. Dam, K. E. Lenox, J. R. Price, and J. M. Storey are with the Oak Ridge National Laboratory, P.O. Box 2008, Oak Ridge, Tennessee 37831. E. A. Wachter and W. G. Fisher are with Galt Technologies, LLC, 2009 Still Water Lane, Knoxville, Tennessee 37922.

Received 14 February 2005; revised manuscript received 29 June 2005; accepted 4 July 2005.

0003-6935/05/337210-08\$15.00/0

© 2005 Optical Society of America

disposable-camera flash tube. The smallest, fielded, scanning imaging lidar system that was found in the literature was based on time-correlated single-photon counting by use of a  $Q$ -switched AlGaAs diode laser with 20 ps pulse widths and providing  $\sim 1$  measurement/s with submillimeter resolution at distances of  $< 10$  m in a  $260 \text{ mm} \times 210 \text{ mm} \times 100 \text{ mm}$  package.<sup>3</sup> In general, the major drawback of narrow-pulse solid-state TOF systems for characterization of anthropogenic aerosols is the necessity for extended measurement intervals owing to low pulse repetition rates.

A variation of the TOF systems is random sequence lidar, for which the laser transmitter beam is intensity modulated with random or pseudorandom codes and the return signal is autocorrelated with the original sequence to determine range or TOF. The advantage of these systems is that they can be implemented in compact, inexpensive packages based on commercially available rf components<sup>4</sup>; however, they also suffer from extended measurement time intervals and cannot measure distributed targets.

A form of lidar that can measure both distributed and hard targets with good spatial resolution and measurement-time intervals over shorter distances is frequency modulated, continuous wave (FM-cw) lidar. FM-cw lidar has been implemented in several forms that basically use a ramped (or chirped) frequency wave that is transmitted toward the target. The backreflected wave scattered from a target is then a delayed version of the transmitted signal. When the return signal is mixed with the transmitted wave, the resultant difference frequency is proportional to the target range (or distance).<sup>5</sup> For lidar systems that frequency modulate by chirping the wavelength of the laser, one can accomplish mixing by heterodyning the return signal with a chirped signal from a second laser (local oscillator) or with a portion of the original transmitted signal obtained from a beam splitter. With both signals incident onto a square law detector such that the two wavefronts are aligned,<sup>6</sup> the output of the detector is the intermediate frequency (i.f.) or difference-frequency signal. The frequency of the i.f. signal is proportional to the target range (distance), and the amplitude is proportional to the scattering strength. Normally a lock-in amplifier (or, alternatively, a spectrum analyzer-fast Fourier transform) is used to extract the frequency and amplitude components of the i.f. signal.

A second category of FM-cw lidar uses intensity modulation, in which the amplitude (rather than the wavelength) of the laser is modulated with a ramped frequency sine wave. Mixing or heterodyning can be performed in the digital domain with a digitized version of the signal that modulates the laser transmitter for the reference or local oscillator signal. Alternatively, mixing can be accomplished by modulation of the bias of a metal-semiconductor-metal detector<sup>7,8</sup> or an image intensifier<sup>9</sup> with an electronic reference signal. The output of the detector is then the i.f. signal.

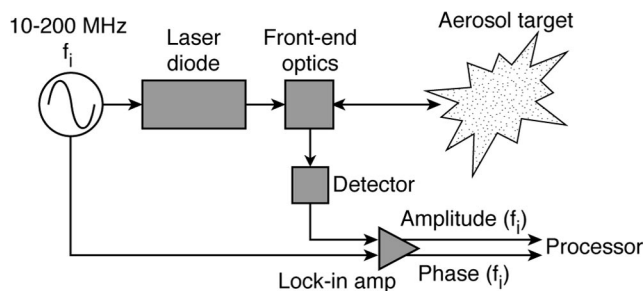


Fig. 1. Schematic of the stepped frequency lidar system. The laser is intensity modulated with a rf signal in 10 MHz steps from 10 to 200 MHz. The amplitude and the phase of the return lidar signal are detected at each frequency by use of a lock-in amplifier, and the resultant vector is then postprocessed to yield range information.

We describe an alternative FM-cw lidar configuration (Fig. 1) that uses discrete stepped, rather than continuously ramped frequency, intensity modulation with lock-in amplifier (or quadrature) detection. As in standard FM-cw lidar, the stepped frequency approach works for both distributed and hard targets. To our knowledge, this approach is new. Measurements are made in the frequency domain, with the analog lock-in amplifier providing phase and amplitude measurements of the return signal at each discrete modulation frequency. Using the lock-in amplifier greatly reduces the amount of data that must be stored and processed compared with that in conventional intensity-modulated schemes. For example, in a typical measurement sequence over a 1 s time interval, the instrument steps through modulation frequencies from 10 to 200 MHz in 10 MHz increments. The output of the lock-in amplifier for a complete measurement cycle is then forty,  $\sim 12$  bit numbers that represent the magnitude and phase of the return signal at each modulation frequency with a corresponding data rate of  $\sim 480$  bits/s. In contrast, conventional FM-cw lidar requires data rates of 2.3 Mbits/s for capturing intermediate frequency signals.<sup>8</sup> In addition, the effective bandwidth of the sub-carrier filter provided by the lock-in amplifier is much narrower than system bandwidths required for capturing intermediate frequencies in conventional FM-cw lidar. The narrower bandwidths provide a large advantage in signal-to-noise ratios (SNRs) for detecting small return signals such as scattering from aerosols. Finally, the stepped frequency implementation takes advantage of current rf commercial off-the-shelf hardware and conventional shorter-wavelength laser diode technology with substantial potential for miniaturization and use in three-dimensional imaging lidar configurations.

In this paper a theory is presented for inverting quadrature signal components from a lock-in amplifier for stepped frequency lidar and determining spatial distributions of single and distributed targets. The resultant spatial scattering intensities are then related to microphysics aerosol models for environmental measurements. Finally, preliminary results

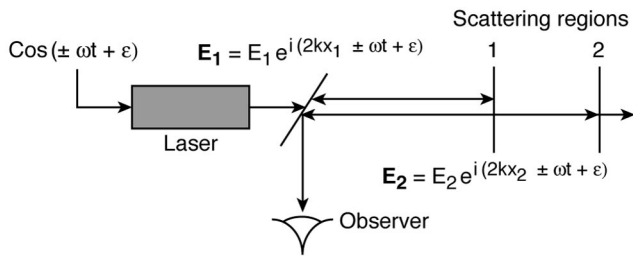


Fig. 2. Complex representation of the modulated lidar signal. Scattering is depicted from two regions in space, resulting in a phase difference in the two return signals. The observer sees a superposition of the two return signal waveforms.

from laboratory measurements with a monostatic FM-cw lidar system with both hard targets and aerosols are discussed.

## 2. Theory

### A. Derivation of Scattering Amplitude Spatial Distributions

A harmonic disturbance traveling in the positive  $x$  direction can be modeled by use of wave vector  $k$ , amplitude  $E_0$ , epoch (or initial) angle  $\varepsilon$ , frequency  $\omega$ , and time  $t$  (Ref. 10):

$$E(x, t) = E_0 \cos(kx \pm \omega t + \varepsilon). \quad (1)$$

For this application,  $E_0$  represents the amplitude of the intensity modulation of the laser beam and  $\omega$  is the modulation frequency. This representation of a traveling wave provides the basis for modeling and processing the signals in intensity-modulated lidar. A simplified schematic of an intensity-modulated lidar system is shown in Fig. 2. In the schematic, scattering is depicted from two points, which are labeled 1 and 2, respectively. The scattered signal from point 1 with round-trip path length  $2x_1$  then has amplitude  $E_1$  and phase shift  $(2kx_1 \pm \omega t + \varepsilon)$ . Likewise, the scattered signal from point 2 has round-trip path length  $2x_2$ , amplitude  $E_2$ , and phase shift  $(2kx_2 \pm \omega t + \varepsilon)$ . The observer sees both scattered signals, and, from the principle of superposition of waves, the resultant wave vector at the observer is

$$\begin{aligned} \mathbf{E}_{\text{obs}} &= E_{\text{obs}} \exp[i(kx \pm \omega t + \varepsilon)] \\ &= E_1 \exp[i(2kx_1 \pm \omega t + \varepsilon)] \\ &\quad + E_2 \exp[i(2kx_2 \pm \omega t + \varepsilon)]. \end{aligned} \quad (2)$$

One technique for extracting phase and amplitude information at the position of the observer is with a lock-in amplifier as shown in Fig. 3. The lock-in amplifier uses the reference signal modulating the intensity of the laser to generate reference sine and cosine waves at the modulation frequency. The sine and cosine waves are then mixed with the measured return lidar signal, resulting in the real and imaginary components of the unknown signal. The square root of the sum of the squares of the real and imag-

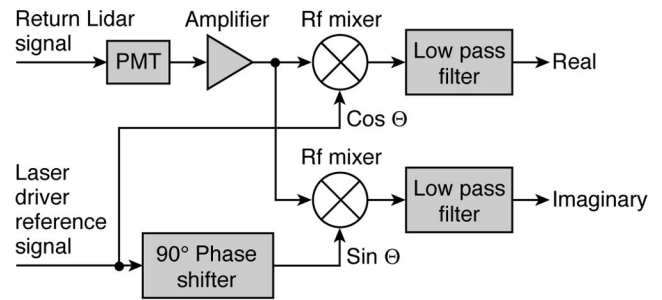


Fig. 3. Schematic of the lock-in amplifier. The signal used to drive the laser provides a reference signal from which sine and cosine waveforms are generated. These sine and cosine reference waveforms are then mixed with the return lidar signal and filtered. The outputs of the lock-in amplifier are then the quadrature components of the return lidar signal from which amplitude and phase can be extracted.

inary components is the amplitude of the lidar signal at the reference frequency. The arc tangent of the ratio of the imaginary and real components is the phase of the lidar signal relative to the reference. Processing the output signal of a detector at the position of an observer using the laser reference signal (frequency  $\omega_0$ ) and a lock-in amplifier yields a measurement vector at the output of the lock-in amplifier of

$$\begin{aligned} \mathbf{E}_{\text{meas}} &= E_{\omega_0} \exp[i(\Theta_{\omega_0})] \\ &= E_1 \exp[i(2kx_1)] + E_2 \exp[i(2kx_2)], \end{aligned} \quad (3)$$

where now  $E_{\omega_0}$  is the amplitude of the superposition of the scattered signals from points 1 and 2 at frequency  $\omega_0$  and  $\Theta_{\omega_0}$  is the phase difference of the composite waveform with respect to the reference signal. For intensity-modulated lidar from a distributed target, the return signal is a superposition of these harmonic waveforms from scattering centers located at several distances  $x_j$ . Equation (3) by itself is underdetermined, and thus one cannot invert it to extract scattering amplitudes  $E_1$  and  $E_2$  at points 1 and 2, respectively. By modulating the laser at a second frequency,  $\omega_1$ , and making measurements of the resultant scattered signals, one can generate a second equation. In general, then, for  $M$  scattering centers (range bins) and  $N$  frequencies and by use of the definition of wave vector  $k$  ( $k = 2\pi/\lambda = \omega/c$ , where  $\lambda$  is the wavelength of the modulation frequency and  $c$  is the speed of light) the following set of equations can be generated:

$$\begin{aligned} E_{\omega_j} \exp[i(\Theta_{\omega_j})] &= \sum_{l=0}^{M-1} E_l \exp\left[i\left(\frac{2\omega_j}{c} x_l\right)\right], \\ j &= 0 \dots N-1. \end{aligned} \quad (4)$$

Equation (4) provide the relationship between the complex amplitudes at the output of the lock-in amplifier at each modulation frequency and the scattering amplitudes at each range bin. To provide range

values in actual distances (e.g., meters) we perform a calibration step with a hard target at a known distance  $x_{\text{ref}}$ . Subsequent measurement vectors are then normalized by the results of the calibration. The normalized scattering function then becomes

$$\begin{aligned} \mathbf{E}_{\text{norm}}(\omega_j) &= E_{\text{norm},\omega_j} \exp[i(\Theta_{\omega_j} - \Theta_{\text{ref},\omega_j})] \\ &= \sum_{l=0}^{M-1} E_{\text{norm},l} \exp\left\{i\left[\frac{2\omega_j}{c}(x_l - x_{\text{ref}})\right]\right\}, \\ j &= 0 \dots N-1, \end{aligned} \quad (5)$$

where  $E_{\text{norm},\omega_j}$  are normalized scattering amplitudes at the detector and  $E_{\text{norm},l}$  are the normalized scattering amplitudes at each range bin,  $x_l$ .

One method of inverting Eq. (5) and extracting the spatial dependence of the scattering amplitudes from measurements in the frequency domain is the inverse Fourier transform. The general form of the inverse Fourier transform is

$$f(x) = \int_{-\infty}^{\infty} F(\beta) \exp[i2\pi\beta x] d\beta. \quad (6)$$

Substituting frequency for variable  $\beta$ , letting  $F(\beta)$  equal the normalized measurement vectors obtained from the lock-in amplifier, and using the kernel  $\exp[i(2\omega/c)(x - x_{\text{ref}})]$  yield the normalized scattering function:

$$E_{\text{norm}}(x) = \int_{-\infty}^{\infty} \mathbf{E}_{\text{norm}}(\omega) \exp\left[i\frac{2\omega}{c}(x - x_{\text{ref}})\right] d\omega. \quad (7)$$

As lock-in amplifier measurements with stepped frequency lidar are discrete and finite, the integral in Eq. (7) can be conveniently expressed in a form much like that of the discrete Fourier transform.<sup>11</sup> For  $N$  frequencies and  $M$  range bins, the discrete, real-valued representation of Eq. (7) can be written as

$$\begin{aligned} E_{\text{norm}}(x_l) &= \frac{1}{N} \sum_{j=0}^{N-1} \text{Re}\left\{E_{\text{norm},\omega_j} \exp[i(\Theta_{\omega_j} - \Theta_{\text{ref},\omega_j})]\right. \\ &\quad \left. \times \exp\left[i\frac{2\omega_j}{c}(x_l - x_{\text{ref}})\right]\right\}, \\ l &= 0 \dots M-1. \end{aligned} \quad (8)$$

Equation (8) is thus a general equation for a stepped frequency, intensity-modulated lidar system that uses quadrature detection and provides normalized scattering amplitudes as a function of distance. The equation is applicable for either single targets or distributed targets (e.g., aerosols). The inputs for Eq. (8) are  $x_{\text{ref}}$  (the distance to the reference target) and the  $N$  measurement vectors (i.e.,  $N$  complex samples) from the lock-in amplifier. Thus, by solving Eq. (8) for a set of  $M$  discrete bins over the measurement range,

one can determine both the amplitude and the location of scattering centers. Note that, with appropriate selections (e.g., power-of-2) for  $N$  and  $M$ , Eq. (8) could be computed with a fast-Fourier-transform algorithm if computational efficiency were a concern. Recall, however, that total scan time increases with the number of frequencies,  $N$ .

The expected shape of the scattering function waveform from Eq. (8) for a single target measured with stepped frequency lidar can be derived by use of a model of the return signal amplitudes in the frequency domain. As described above, the lock-in amplifier produces complex amplitude vectors (amplitude and phase) at each modulation frequency. The amplitude signals determine the scattering strength(s) of the target(s), and the phase signals determine location by means of the scattering function in Eq. (8). The normalized amplitudes of the return signal at different frequencies for a fixed-location, single target are constant (modulating the laser at different frequencies does not change the intensity of the return signal). In frequency space the return signal amplitudes can thus be modeled as a rectangle function with width proportional to the modulation bandwidth. We define a one-dimensional rectangle function<sup>12</sup> as

$$G(f) = A \text{rect}\left(\frac{f-f_0}{b}\right) = \begin{cases} 0 & \left|\frac{f-f_0}{b}\right| > \frac{1}{2} \\ \frac{A}{2} & \left|\frac{f-f_0}{b}\right| = \frac{1}{2} \\ A & \left|\frac{f-f_0}{b}\right| < \frac{1}{2} \end{cases}, \quad (9)$$

where  $f$  is the independent variable along the frequency axis,  $f_0$  determines the position of the rectangle function on the axis,  $b$  is a scaling function that is proportional to width, and  $A$  is the height. For stepped frequency cw lidar,  $f_0$  represents the center frequency of modulation,  $b$  is a constant that is proportional to the modulation bandwidth or range of frequencies used in the measurement, and  $A$  represents the scattering amplitude.

The inversion algorithm, Eq. (8), is an inverse Fourier transform of the lock-in amplifier measurements in frequency space. Taking the finite inverse Fourier transform of Eq. (13) yields

$$\begin{aligned} g(x) &= \int_{-\infty}^{\infty} G(f) \exp(i2\pi xf) df \\ &= Ab \text{sinc}(bx) \exp(i2\pi xf_0). \end{aligned} \quad (10)$$

The amplitude of Eq. (10) is plotted in Fig. 4. The resultant sinc function has a width that is inversely proportional to the modulation bandwidth and an amplitude that is proportional to the scattering strength. The FWHM of the curve occurs at  $1/2b$  and corresponds to the expected range resolution in traditional

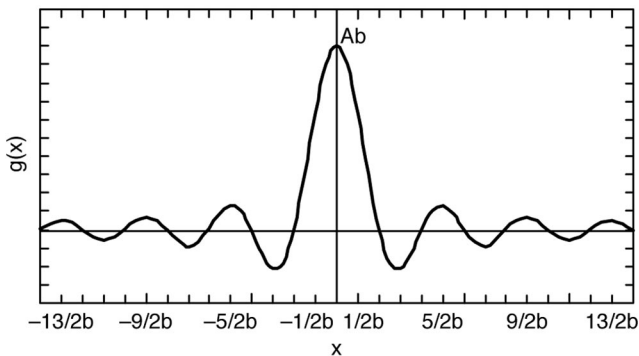


Fig. 4. Expected return signal waveform (postprocessing) for a single target from a stepped frequency lidar is a sinc function with amplitude proportional to the backscatter signal amplitude and width inversely proportional to twice the modulation bandwidth. The FWHM of the sinc function determines the range resolution of the lidar system.

FM-cw lidar, which is  $c/2\Delta f$ , where  $c$  is the speed of light ( $3 \times 10^8$  m/s) and  $\Delta f$  is the modulation bandwidth.

#### B. Relationship of System's Signal-to-Noise Ratio and Aerosol Backscatter Coefficient

Here, the equations for the system's SNR are derived and related to aerosol backscatter coefficients. Aerosol emissions from heavy-duty vehicles can be characterized by a well-defined range of reflectivities and sizes. The size distribution after emission changes with time, but the time scale (of the order of seconds) is long enough to allow for measurements. With lidar, one can measure aerosol backscatter coefficients by transmitting a laser signal and measuring the amount of signal returned owing to scattering from the aerosols.

In general, laser light interacts with aerosols by absorption and scattering. By assuming spherical aerosol particles and using Mie theory<sup>13</sup> and by knowing the wavelength of the laser light, the effective refractive index of the particles, and the particle sizes and size distribution, one can derive a theoretical

tics of the processing electronics, one can determine how much light was returned and therefore the total backscatter coefficient of an aerosol plume.

An intensity-modulated lidar system is analogous to a category of optical communication systems that uses subcarrier direct detection receivers. These communication systems intensity modulate an optical carrier that has a characteristic optical wavelength, with a high-frequency radio subcarrier wave. Information is transmitted in this type of communication system by modulation of the rf subcarrier wave. The equation used for relating the measured lidar signal to an aerosol backscatter coefficient is therefore based on the equation for the SNR of a subcarrier direct detection receiver<sup>14</sup>:

$$\text{SNR}_{\text{receiver}} = \frac{[G(\eta q/hf)]^2 P_{\text{sig}}^2 R_L}{16G^2 q \{ (\eta q/hf) [(P_{\text{sig}}/2) + P_{\text{bkg}}] + I_{\text{drk}} \} BR_L + 32kTB} \quad (11)$$

where  $G$  is the photodetector's current gain,  $R_L$  is the optical receiver's load resistance,  $P_{\text{sig}}$  is the return signal power,  $P_{\text{bkg}}$  is the background power,  $I_{\text{drk}}$  is the photodetector's dark current,  $\eta$  is the detector efficiency,  $q$  is the charge on an electron,  $k$  is Boltzmann's constant,  $h$  is Planck's constant,  $f$  is the frequency of the laser light ( $c/\lambda$ ),  $T$  is temperature in degrees kelvin, and  $B$  is the effective bandwidth of the subcarrier filter provided by the lock-in amplifier. The return signal power at the receiver can then be derived from the transmitted power of the laser  $P_{\text{laser}}$ , the backscatter coefficient of the aerosols, the overall lidar system efficiency including the detector  $\eta_{\text{sys}}$ , and the optical receiver parameters  $\Omega_{\text{opt}}$ :

$$\eta P_{\text{sig}} = \eta_{\text{sys}} P_{\text{laser}} \beta \Omega_{\text{opt}} \quad (12)$$

Now, combining Eqs. (11) and (12), one can derive a system's SNR (which includes detector, optics, atmospheric effects, and electronics):

$$\text{SNR}_{\text{system}} = \frac{[G(\eta_{\text{sys}} q/hf)]^2 P_{\text{laser}}^2 \beta^2 \Omega_{\text{opt}}^2 R_L}{16G^2 q \{ (q/hf) [(\eta_{\text{sys}} P_{\text{laser}} \beta \Omega_{\text{opt}}/2) + \eta P_{\text{bkg}}] + I_{\text{drk}} \} BR_L + 32kTB} \quad (13)$$

volume backscatter coefficient (analogous to the reflectivity of a hard target surface). The amount of light scattered backward from an aerosol plume can then be theoretically calculated from this coefficient.

The volume backscatter coefficient,  $\beta$ , is thus the parameter that is measured with the lidar system and related to the aerosol microphysics models. By deriving the lidar transfer function, which includes the amount of power transmitted from the laser, the solid angle subtended by the receiving optics, the efficiency of the detector, and the noise characteris-

Therefore, given a set of optical system parameters, Eq. (13) provides the theoretical lidar system response linking the SNR and volume backscatter coefficient,  $\beta$ . For shot-noise-limited operation, Eq. (13) reduces to

$$\text{SNR}_{\text{system}} = \frac{\eta_{\text{sys}} P_{\text{laser}} \beta \Omega_{\text{opt}}}{8hfB} \quad (14)$$

In a typical lidar system, one obtains measure-

ments of the SNR by dividing the measured signal power of a return lidar pulse by a background measurement (no signal).<sup>15</sup> For stepped frequency lidar, the inversion process in Eq. (8) provides signal amplitude as a function of distance, which must then be squared to equate to signal power. In addition, for the smaller signals obtained from aerosol scattering, subtracting a background measurement from the signal's amplitude before squaring is necessary. Thus the equation used to convert normalized scattering amplitudes for  $M$  range bins into measured SNR values is

$$\text{SNR}_{\text{meas}}(x_k) = \frac{[E_{\text{norm-meas}}(x_k) - E_{\text{norm-bkg1}}(x_k)]^2}{\frac{1}{M} \sum_k [E_{\text{norm-bkg2}}(x_k) - E_{\text{norm-bkg1}}(x_k)]^2}, \quad (15)$$

where  $E_{\text{norm-meas}}(x_k)$ ,  $E_{\text{norm-bkg1}}(x_k)$ , and  $E_{\text{norm-bkg2}}(x_k)$  are the scattering functions calculated from Eq. (8) for the aerosol measurement and two background measurements, respectively. Note that the background measurements depend on  $x_k$ .

### 3. Laboratory Measurements

#### A. Single- and Multiple-Target Scattering with Translucent Targets

To demonstrate the ability of intensity-modulated stepped frequency cw lidar to perform distributed measurements, we performed a series of experiments using a monostatic lidar system with translucent targets. In the tests, measurements were made with single and multiple clear plastic targets at known locations. The target ranges measured by the lidar system were then compared to the known locations.

A monostatic lidar unit was designed and built to test the intensity-modulated, stepped frequency lidar concept in the lab. The lidar system uses a Hitachi Model HL6501MG 660 nm laser diode, which is modulated from 10 to 200 MHz in 10 MHz steps. The lower modulation frequency (10 MHz) was chosen to provide an unambiguous system measurement range of 30 m. The photodetector is a Hamamatsu Model H5783-01 photomultiplier tube, and the rf lock-in amplifier is a Stanford Research Systems Model SR844 (with an internal, user-programmable reference waveform generator).

Initial measurements with the system were made with single and multiple targets that could be positioned relative to the primary lens by means of an optical rail. The targets are 5 cm × 5 cm × 1 mm transparent plastic sheets that are aligned in parallel along the length of an optical rail. Figure 5 shows a typical waveform obtained from a single clear plastic target by use of the stepped frequency lidar system. As expected from the analysis, the general shape of the processed return signal is a sinc function with its peak at the target location. For the waveform in Fig. 5, the plastic target was located 2.5 m from the primary lens. In addition, tests were performed with

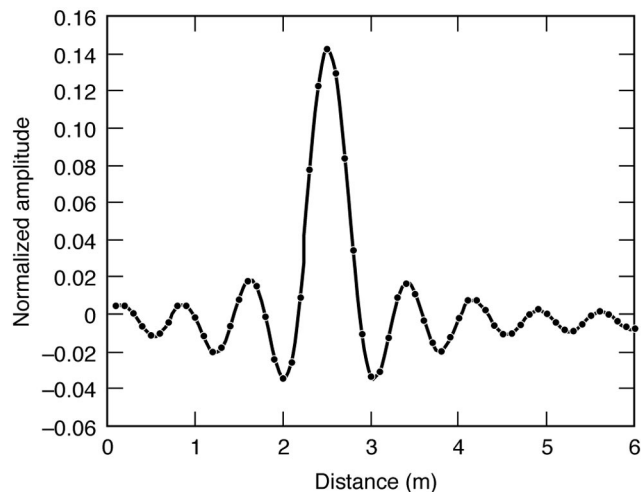


Fig. 5. Processed scattering waveform from a single translucent target located 2.5 m from the stepped frequency lidar system. The return signal is a sinc function as expected and has a spatial resolution of 0.75 m (FWHM), corresponding to a modulation bandwidth of 190 MHz.

multiple plastic targets along the length of the optical rail. Figure 6 shows a typical waveform obtained with four clear plastic targets at locations given in the figure. The resultant waveform is the superposition of four sinc functions. Tests were also performed in which the distance between two targets was varied to quantify range resolution. It was found that if the distance between two targets was less than ~0.75 m, the two waveforms merged and were not distinguishable. This value corresponds to the  $c/2\Delta f$  theoretical range resolution of 0.789 m, given a modulation bandwidth of 190 MHz.

#### B. Aerosol Particle Measurements

For the aerosol experiments, size distribution(s) of the aerosol stream(s) are measured as follows, before the lidar measurements: A TSI scanning mobility

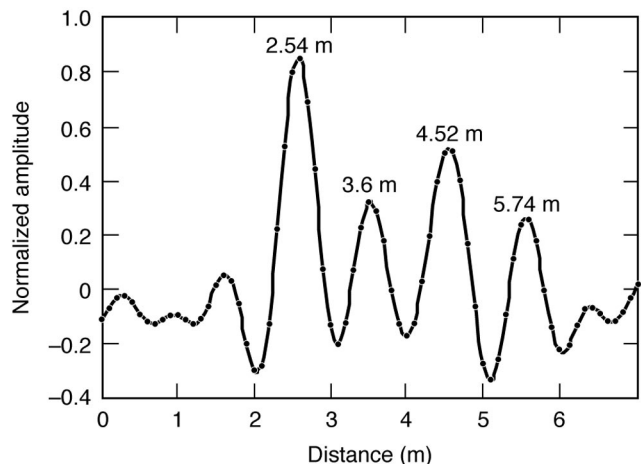


Fig. 6. Normalized scattering waveform (postprocessing) from multiple translucent targets, demonstrating the capability of stepped frequency lidar to measure distributed targets. The actual target locations are provided above the peaks.

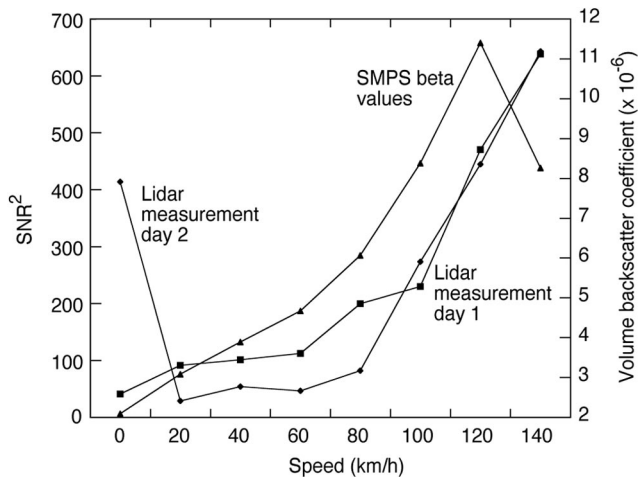


Fig. 7. Results from a laboratory diesel engine test, demonstrating the correlation between calculated beta values from sampled SMPS data and lidar SNR measurements, shown on a dual-axis plot. The lidar results are from measurements made on two separate days. The larger value of SNR at 0 km/h on day 2 is due to a cold engine start.

particle spectrometer (SMPS) equipped with a differential mobility analyzer (TSI long direct memory access A model) was used to classify the size of the particles, while a TSI ultrafine condensation particle counter was used to count the number of particles classified by direct memory access. Each measurement of a particle size distribution from 10 to 400 nm took 4 min. The SMPS sheath to aerosol flow rate was operated at a 10:1 ratio. The sample for the SMPS is obtained with a probe placed into the aerosol stream before and after light-scattering data are taken.

To calculate the volume backscatter coefficient for the aerosol as a whole, we first calculated the coefficient for the individual particle sizes from SMPS data. This single-particle scattering efficiency or cross section is derived from Mie theory for a spherical particle of known particle size (diameter) and complex refractive index. The refractive index for an ammonium sulfate aerosol, for instance, has a real number 1.521 and an imaginary part of 0 measured at a wavelength of 589 nm.<sup>16</sup> For carbon particles in diesel exhaust we used a refractive-index value of  $1.96 + 0.66i$ . We used 32 size bins of the SMPS data for the Mie calculation. The midpoint of each bin was then used as the diameter for the entire bin. Then the single-particle scattering cross section was multiplied by the number concentration of particles for a given bin size measured by SMPS (there were  $N_i$  particles in the  $i$ th bin) and the product was integrated over the whole SMPS size distribution to yield the volume backscatter coefficient.<sup>17</sup>

We performed an initial laboratory test with the stepped frequency lidar system to measure a plume of exhaust from a light-duty diesel vehicle driving on a chassis dynamometer. Measurements were made on two separate days, and SNR values calculated from Eq. (15) were recorded for engine speeds from 0 to 140 km/h. The lidar instrument was located ap-

proximately 1.75 m from the exhaust plume. In addition, we took one set of SMPS data at each engine speed by sampling the exhaust, and the resultant data were correlated to beta values by use of microphysics models as described above. In Fig. 7 the results of the diesel engine tests are shown in a dual-axis plot. In the figure, peak values of SNR obtained from lidar measurements are compared with the beta values obtained from SMPS data. There is good correlation in the general trends of the SNR and SMPS data. The initial high value of the SNR data point at 0 km/h on day 2 of the test was the result of a cold engine start. The reason for the lower value of SMPS data at 140 km/h is not known. In contrast, both lidar measurements showed an increase in scattering intensity at 140 km/h, as expected. To quantitatively compare the lidar and SMPS data, further study to characterize the optical system parameters by use of standardized aerosols and aerosol distributions is needed.

#### 4. Conclusions

In this paper an alternative intensity-modulated FM cw lidar system for making distributed measurements of aerosols and multiple hard targets was described. The system is based on stepped frequency modulation with quadrature detection and has the advantages of using commercially available rf components, enhancing the measurement SNR, and greatly reducing the amount of data that must be stored and processed compared with conventional intensity and phase modulation schemes. The equations for processing stepped frequency lidar signals were derived, and laboratory measurements and initial results from both hard targets and aerosols were presented. The potential for both miniaturizing the existing platform and developing imaging array sensors for plume characterization was described. Future efforts at the Oak Ridge National Laboratory will concentrate on a rigorous characterization of the stepped frequency lidar system by using standard aerosols with known size distributions as well as measurements of exhaust products and emissions from diesel and jet engines in laboratory and in field settings.

#### References

1. K. E. Lenox, A. Akerman, C. W. Ayers, T. Q. Dam, S. Goe-deke, R. N. McGill, J. M. Storey, M. Cheng, R. K. Richards, M. L. Simpson, W. G. Fisher, and E. A. Wachter, "Further development of remote sensing instrumentation for NO<sub>x</sub> and PM emissions from heavy duty trucks," in *Proceedings Air and Waste Management 96th Annual Conference*, A. Knopes, ed. (Air and Waste Management Association, 2003), paper 69731.
2. J. E. Nettleton, B. W. Schilling, D. N. Barr, and J. S. Lei, "Monoblock laser for a low-cost, eyesafe, microlaser range finder," *Appl. Opt.* **39**, 2428–2432 (2000).
3. J. Massa, G. Buller, A. Walker, G. Smith, S. Cova, M. Uma-suthan, and A. Wallace, "Optical design of three-dimensional imaging and ranging system based on time-correlated, single-photon counting," *Appl. Opt.* **41**, 1063–1070 (2002).
4. M. Bashkansky, H. R. Burris, E. E. Funk, R. Mahon, and C. I.

- Moore, "RF phase-coded random-modulation LIDAR," *Opt. Commun.* **231**, 93–98 (2004).
5. R. B. Chadwick and R. G. Strauch, "Processing of FM-cw Doppler radar signals from distributed targets," *IEEE Trans. Aerosp. Electron. Syst.* **AES-15**, 185–188 (1979).
  6. M. L. Simpson, C. A. Bennett, M. S. Emery, D. P. Hutchinson, G. H. Miller, R. K. Richards, and D. N. Sitter, "Coherent imaging with two-dimensional focal-plane arrays: design and application," *Appl. Opt.* **36**, 6913–6920 (1997).
  7. B. L. Stann, W. C. Ruff, and Z. G. Sztankay, "Intensity-modulated diode laser radar using frequency-modulation/continuous-wave ranging techniques," *Opt. Eng.* **35**, 3270–3278, (1996).
  8. B. Stann, A. Abou-Auf, K. Aliberti, M. Giza, B. Ovrebo, W. Ruff, D. Simon, and M. Stead, "Research progress on scannerless ladar systems using a laser diode transmitter and FM/cw radar principles," in *Aerosense 2002 Laser Radar Technology and Applications VII*, G. W. Kamerman, ed., *Proc. SPIE* **4723** 4723–4733, (2002).
  9. R. L. Schmitt, R. J. Williams, and J. D. Matthews, "High-frequency scannerless imaging laser radar for industrial inspection and measurement applications," Rep. SAND96-2739 (Sandia National Laboratory, 1996).
  10. E. Hecht, *Optics* (Addison-Wesley, 1987), pp. 12–21 and 246–247.
  11. A. V. Oppenheim and R. W. Schaffer, *Discrete-Time Signal Processing* (Prentice-Hall, 1989), pp. 514–561.
  12. J. D. Gaskill, *Linear Systems, Fourier Transforms, and Optics* (Wiley, 1978), p. 181.
  13. H. C. van de Hulst, *Light Scattering by Small Particles* (Wiley, 1957).
  14. W. K. Pratt, *Laser Communications Systems* (Wiley, 1969), pp. 178–183.
  15. J. Rothermel, D. M. Chambers, M. A. Jarzembski, V. Srivastava, D. A. Bowdle, and W. D. Jones, "Signal processing and calibration of continuous-wave focused CO<sub>2</sub> Doppler lidars for atmospheric backscatter measurement," *Appl. Opt.* **35**, 2083–2095 (1996).
  16. J. H. Seinfeld and S. N. Pandis, *Atmospheric Chemistry and Physics* (Wiley, 1998), p. 1118.
  17. C. F. Bohren and D. R. Huffman, *Absorption and Scattering of Light by Small Particles* (Wiley, 1983), p. 589.